Acta Cryst. (1999). B**55**, 246–254

Anhydrous ammonioguanidinium(2+) and dihydrated bis[aminoguanidinium(1+)] hexafluorosilicates†: new co-products of preparing ferroelectric ammonioguanidinium(2+) hexafluorozirconate

C. R. Ross II,[a] M. R. Bauer,[b] R. M. Nielson[b] and S. C. Abrahams[c]*

[a]*Department of Structural Biology, St. Jude Children's Research Hospital, 332 North Lauderdale St., Memphis, TN 38105-2794, USA,* [b]*Chemistry Department, Southern Oregon University, Ashland, OR 97520, USA, and* [c]*Physics Department, Southern Oregon University, Ashland, OR 97520, USA. E-mail: sca@mind.net*

(*Received 14 May 1998; accepted 9 October 1998*)

Abstract

Ammonioguanidinium hexafluorosilicate, $CH_8N_4^{2+}\cdot SiF_6^{2-}$, and bis(aminoguanidinium) hexafluorosilicate dihydrate, $2CH_7N_4^{+}\cdot SiF_6^{2-}\cdot 2H_2O$, are new materials formed as by-products in course of preparing ferroelectric $CH_8N_4ZrF_6$ in the presence of glassware. Their structures were determined for comparison with the corresponding hexafluorozirconates. All atoms including the eight H atoms in the $CH_8N_4^{2+}$ cation and the seven H atoms in the $CH_7N_4^{+}$ cation have been located and refined with $wR(F^2) = 0.0653$, $R = 0.0255$, $S = 1.146$ and $wR(F^2) = 0.0745$, $R = 0.0301$, $S = 1.065$, respectively. The N_2C-N-N backbone of the 2+ cation is close to planarity, while that of the 1+ cation does not differ significantly from planarity. The SiF_6^{2-} octahedron is nearly ideally regular in both materials, with <Si—F> = 1.684 (unbiassed estimator of standard uncertainty = 0.016) Å in the anhydrous hexafluorosilicate and 1.6801 (unbiassed estimator of standard uncertainty = 0.0006) Å in the dihydrate. The combination of coulombic and NH···F interactions in $CH_8N_4SiF_6$ results in a relatively dense variant of the NaCl structure. In addition to similar forces, the dihydrate is also characterized by the role of the water molecule with its strong NH···O interactions; its packing efficiency is, however, appreciably less than that of the anhydrous hexafluorosilicate with an ∼8% increase in void space. Cleaved crystals of the dihydrate are frequently twinned across the (001) composition plane, with a twofold rotation about the *b* axis as the twin operation.

1. Introduction

Preparation of ferroelectric ammonioguanidinium(2+) hexafluorozirconate, $CH_8N_4ZrF_6$, by reaction in aqueous solution is generally accompanied by formation of a variety of related compositions. Among these is the monohydrate $CH_8N_4ZrF_6\cdot H_2O$, the crystal structure of which contains distorted antiprisms of edge-sharing ZrF_8 as the repeating structural unit (Bukvetskii *et al.*, 1989; Ross *et al.*, 1998). Short segments of ZrF_8 antiprisms in the monohydrate fold back to form four-membered rings; by contrast, distorted antiprisms of ZrF_8 in ferroelectric $CH_8N_4ZrF_6$ join to form infinite chains (Bukvetskii *et al.*, 1990). Other compositions include the semihydrate $CH_8N_4ZrF_6\cdot\frac{1}{2}H_2O$, which contains edge-sharing pairs of ZrF_7 and ZrF_8 polyhedra (Gerasimenko *et al.*, 1986), bis[aminoguanidinium(1+)] hexafluorozirconate, $(CH_7N_4)_2ZrF_6$, with its individual ZrF_6 octahedra and lack of shared F atoms (Bukvetskii *et al.*, 1990), aminoguanidinium(1+) pentafluorozirconate, $CH_7N_4ZrF_5$, with its infinite chains of polyhedra (Bukvetskii *et al.*, 1992; Ross *et al.*, 1999), bis[guanidinium(1+)] hexafluorozirconate, $(CH_6N_3)_2ZrF_6$, with edge-sharing pairs of ZrF_7 polyhedra (Bukvetskii *et al.*, 1987) and $ZrF_4\cdot HF\cdot 3H_2O$, the powder pattern but not the structure of which has been reported, in addition to the formation of $ZrF_4\cdot 2HF\cdot 0.7H_2O$, $ZrF_4\cdot HF\cdot 1.5H_2O$, and $ZrF_4\cdot 3H_2O$ (Waters, 1960).

Clarification of the specific conditions required for preparing pure ferroelectric ammonioguanidinium(2+) hexafluorozirconate, in addition to interest in the reactions leading to the unexpected formation of two previously unknown hexafluorosilicates, led to determination of the title crystal structures and consideration of the differences between them as reported herein.

2. Experimental

2.1. *Preparation and crystal growth of anhydrous ammonioguanidinium(2+) hexafluorosilicate*

Colorless crystals of the new material $CH_8N_4SiF_6$ were initially recognized morphologically in the course of attempts to prepare ferroelectric $CH_8N_4ZrF_6$ by methods that included use of glassware at two separate

† The systematic names of the compounds studied in this paper are given following IUPAC recommendations. The corresponding fluorozirconates have previously been referred to in the literature by the non-IUPAC names aminoguanidinium(2+) hexafluorozirconate and diaminoguanidinium(1+) hexafluorozirconate for ammonioguanidinium(2+) hexafluorozirconate and bis[aminoguanidinium(1+)] hexafluorozirconate, respectively.

stages; their prismatic morphology, with characteristically extended faces, differed markedly from previous preparations. Preliminary diffraction examination revealed a unit cell that could not be found in the literature. The possibility that Si might have become substituted for Zr in this preparation was checked by examining the results of a reaction between 4.6 mmol SiO_2 (Aldrich, 99.9%) and excess (60 mmol) HF aqueous solution (Aldrich, 48–51%) in a polypropylene beaker, followed by heating for 1 h in a bath of boiling water followed by separately dissolving 4.6 mmol aminoguanidine bicarbonate (Aldrich, 98.5%) in 9.2 mmol HF solution also in a polypropylene beaker. Combination of the two solutions, followed by reduction in volume to ~5% in a boiling-water bath, gave transparent crystals with a maximum length of 6 mm and a cross section of about 0.5 × 0.5 mm. The resulting unit-cell dimensions matched those of the accidentally grown crystals. A preliminary structure determination confirmed their composition as $CH_8N_4SiF_6$. It may be noted that formation of anhydrous $CH_8N_4SiF_6$ requires a large excess of HF.

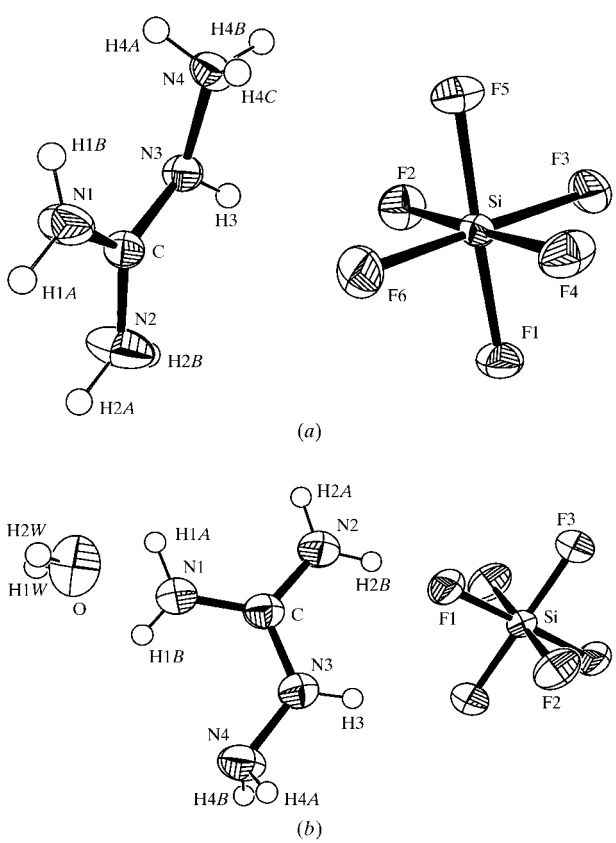

Fig. 1. (*a*) *ORTEP* (Burnett & Johnson, 1996) plot of $CH_8N_4SiF_6$ with the atomic labeling. Displacement ellipsoids are drawn at the 50% probability level. (*b*) *ORTEP* plot of $(CH_7N_4)_2SiF_6{\cdot}2H_2O$ with the atomic labeling. Displacement ellipsoids are drawn at the 50% probability level.

2.2. *Preparation and crystal growth of bis[aminoguanidinium(1+)] hexafluorosilicate dihydrate*

$(CH_7N_4)_2SiF_6{\cdot}2H_2O$ was prepared by adding 4.6 mmol SiO_2 (Aldrich, 99.9%) to 27.5 mmol HF aqueous solution (Aldrich, 48–51%) in a 50 ml digestion bomb. After rinsing the top inside walls with 5 ml water, the bomb was sealed and heated to 428 K for 72 h, then cooled to room temperature thereby forming H_2SiF_6 aqueous solution. Following the addition of 9.2 mmol aminoguanidine bicarbonate (Aldrich, 98.5%) to the solution, the bomb was reheated to 403 K for 3 h and cooled to room temperature. Transfer of the resulting solution to a polypropylene beaker led overnight to crystallization. All crystals produced were transparent colorless prisms with maximum dimensions of about 0.5 mm. Major prism faces are (001) and (101) with elongation direction [010]. A preliminary structure determination revealed their composition to be $(CH_7N_4)_2SiF_6{\cdot}2H_2O$.

2.3. *Structure determination and refinement of anhydrous ammonioguanidinium(2+) hexafluorosilicate*

The cleavage fragment studied was mounted in nail polish (to prevent air contact) on an Enraf–Nonius MACH3 diffractometer. Reflections for unit-cell dimensions were centered at four independent settings to eliminate encoder errors by the *SET*-4 procedure (Enraf–Nonius, 1988). See Table 1 for all other experimental details.†

The structure was solved using *SIR*92 (Burla *et al.*, 1989), with all heavy atoms apparent in the initial map. The resulting structure was refined on F^2_{obs} using *SHELX*97.1 (Sheldrick, 1997), with weights initially proportional only to counting statistics. Difference Fourier maps following several refinement cycles revealed the positions of all H atoms, which were thereupon added to the model under the following initial constraints: d_{N-H} = 0.89 Å about N4, all other d_{N-H} = 0.86 Å, bond angles about N4 constrained to regular tetrahedral values, NH_2 groups constrained flat and in the molecular plane of the ammonioguanidinium cation and N3—H bisecting the external C—N3—N4 angle; see Fig. 1(*a*) for the atomic labeling. Examination of paired F^2_{obs} and F^2_{calc} values indicated the significant presence of extinction, hence an extinction parameter was included in the refinement. The extinction correction used was of the form $k[1 + 0.001xF^2_{calc}\lambda^3/\sin(2\theta)]^{-1/4}$, where k is the overall scale factor and x is a refinable parameter (Sheldrick, 1997). The final weighting scheme is given in Table 1, where the first term represents counting statistics and the coefficients of $P = (F^2_{obs} + 2F^2_{calc})/3$ are based on analysis of variance.

† Supplementary data for this paper are available from the IUCr electronic archives (Reference: BR0080). Services for accessing these data are described at the back of the journal.

Table 1. *Experimental details*

Crystal data		
Chemical formula	$CH_8N_4^{2+}{\cdot}SiF_6^{2-}$	$2CH_7N_4^{+}{\cdot}SiF_6^{2-}{\cdot}2H_2O$
Chemical formula weight	218.2	328.33
Cell setting	Orthorhombic	Triclinic
Space group	*Pccn*	$P\overline{1}$
a (Å)	10.4232 (1)	6.5124 (1)
b (Å)	17.6675 (2)	6.6952 (2)
c (Å)	7.5363 (1)	8.0215 (3)
α (°)	90	70.723 (2)
β (°)	90	82.745 (2)
γ (°)	90	89.243 (3)
V (Å^3)	1387.82 (3)	327.348 (16)
Z	8	1
D_x (Mg m^{-3})	2.089	1.666
D_m (Mg m^{-3})	2.11 (3)	1.67 (1)
Density measured by	Pycnometry	Pycnometry
Radiation type	Cu $K\alpha$	Cu $K\alpha$
Wavelength (Å)	1.5418	1.5418
No. of reflections for cell parameters	24	25
θ range (°)	42.5–47.5	42.5–47.5
μ (mm^{-1})	3.888	2.487
Temperature (K)	293 (2)	293 (2)
Crystal form	Blocky	Prismatic
Crystal size (mm)	0.29 × 0.17 × 0.16	0.35 × 0.31 × 0.17
Crystal color	Colorless, clear	Colorless, clear
Data collection		
Diffractometer	MACH3	MACH3
Data collection method	ω–2θ scans	ω–2θ scans
Absorption correction	Analytical	Analytical
T_{min}	0.415	0.45
T_{max}	0.595	0.61
No. of measured reflections	3143	2404
No. of independent reflections	1315	1239
No. of observed reflections	1267	1224
Criterion for observed reflections	$I > 2\sigma(I)$	$I > 2\sigma(I)$
R_{int}	0.0191	0.0268
θ_{max} (°)	69.73	69.79
Range of h, k, l	$-12 \rightarrow h \rightarrow 12$	$-7 \rightarrow h \rightarrow 7$
	$-1 \rightarrow k \rightarrow 21$	$-8 \rightarrow k \rightarrow 8$
	$-1 \rightarrow l \rightarrow 9$	$-9 \rightarrow l \rightarrow 9$
No. of standard reflections	3	3
Frequency of standard reflections	Every 60 min	Every 60 min
Intensity decay (%)	7	5
Refinement		
Refinement on	F^2	F^2
$R[F^2>2\sigma(F^2)]$	0.0255	0.0301
$wR(F^2)$	0.0653	0.0745
S	1.146	1.065
No. of reflections used in refinement	1315	1239
No. of parameters used	142	125
H-atom treatment	All H-atom parameters refined	All H-atom parameters refined
Weighting scheme	$w = 1/[\sigma^2(F_o^2) + (0.0340P)^2 + 0.4906P]$ where $P = (F_o^2 + 2F_c^2)/3$	$w = 1/[\sigma^2(F_o^2) + (0.0295P)^2 + 0.1278P]$ where $P = (F_o^2 + 2F_c^2)/3$
$(\Delta/\sigma)_{max}$	0.001	0.001
$\Delta\rho_{max}$ (e Å^{-3})	0.215	0.284
$\Delta\rho_{min}$ (e Å^{-3})	−0.307	−0.219
Extinction method	*SHELX*97 (Sheldrick, 1997)	*SHELX*97 (Sheldrick, 1997)
Extinction coefficient	0.0076 (4)	0.043 (4)
Source of atomic scattering factors	*International Tables for Crystallography* (1992, Vol. C, Tables 4.2.6.8 and 6.1.1.4)	*International Tables for Crystallography* (1992, Vol. C, Tables 4.2.6.8 and 6.1.1.4)
Computer programs		
Data collection and cell refinement	*CAD*-4 *EXPRESS* (Enraf–Nonius, 1988)	*CAD*-4 *EXPRESS* (Enraf–Nonius, 1988)
Data reduction	*XCAD*-4 (Harms, 1997); *ABSPSI* (Alcock & Marks, 1994)	*XCAD*-4 (Harms, 1997); *ABSPSI* (Alcock & Marks, 1994)

Table 2. *Fractional atomic coordinates and equivalent isotropic displacement parameters (Å^2) for $CH_8N_4SiF_6$*

$U_{eq} = (1/3)\Sigma_i\Sigma_j U^{ij} a^i a^j \mathbf{a}_i.\mathbf{a}_j$.

	x	y	z	U_{eq}
Si	0.45067 (3)	0.36631 (2)	0.61337 (5)	0.01893 (15)
F1	0.53956 (8)	0.42962 (5)	0.72439 (12)	0.0304 (2)
F2	0.39434 (9)	0.43412 (5)	0.48043 (12)	0.0324 (2)
F3	0.32849 (8)	0.38265 (6)	0.75852 (12)	0.0357 (2)
F4	0.50423 (9)	0.29678 (5)	0.75149 (12)	0.0357 (2)
F5	0.35997 (8)	0.30235 (5)	0.50833 (11)	0.0311 (2)
F6	0.57320 (9)	0.34800 (6)	0.47477 (12)	0.0376 (3)
C	0.61530 (13)	0.40105 (8)	0.10974 (18)	0.0236 (3)
N1	0.66326 (14)	0.33835 (8)	0.0451 (2)	0.0353 (3)
H1*A*	0.744 (3)	0.3375 (13)	0.028 (3)	0.051 (6)
H1*B*	0.617 (3)	0.3107 (16)	−0.008 (4)	0.074 (8)
N2	0.68857 (15)	0.45801 (9)	0.1506 (3)	0.0457 (4)
H2*A*	0.773 (3)	0.4530 (13)	0.133 (3)	0.055 (6)
H2*B*	0.657 (2)	0.4968 (15)	0.181 (3)	0.055 (7)
N3	0.48640 (12)	0.40978 (7)	0.13244 (17)	0.0236 (3)
H3	0.4682 (18)	0.4359 (11)	0.206 (3)	0.030 (5)
N4	0.40871 (12)	0.34376 (7)	0.12861 (19)	0.0258 (3)
H4*A*	0.396 (2)	0.3328 (12)	0.025 (3)	0.042 (6)
H4*B*	0.332 (2)	0.3565 (13)	0.173 (3)	0.052 (6)
H4*C*	0.441 (2)	0.3017 (14)	0.186 (3)	0.057 (6)

Table 3. *Fractional atomic coordinates and equivalent isotropic displacement parameters (Å^2) for $(CH_7N_4)_2SiF_6{\cdot}2H_2O$*

$U_{eq} = (1/3)\Sigma_i\Sigma_j U^{ij} a^i a^j \mathbf{a}_i.\mathbf{a}_j$.

	x	y	z	U_{eq}
Si	0	0	0	0.0310 (2)
F1	0.04859 (14)	−0.01478 (16)	0.20441 (12)	0.0478 (3)
F2	0.12778 (16)	0.23518 (15)	−0.08741 (14)	0.0543 (3)
F3	−0.22230 (14)	0.12017 (16)	0.03280 (13)	0.0531 (3)
C	0.4773 (2)	0.2381 (2)	0.5241 (2)	0.0344 (3)
N1	0.5514 (2)	0.1627 (2)	0.67681 (19)	0.0442 (3)
H1*A*	0.465 (3)	0.116 (3)	0.777 (3)	0.046 (5)
H1*B*	0.671 (3)	0.151 (3)	0.679 (2)	0.037 (5)
N2	0.2754 (2)	0.2442 (3)	0.5163 (2)	0.0461 (4)
H2*A*	0.182 (3)	0.193 (3)	0.610 (3)	0.054 (5)
H2*B*	0.235 (3)	0.294 (3)	0.417 (3)	0.045 (5)
N3	0.6031 (2)	0.3118 (2)	0.37175 (19)	0.0408 (3)
H3	0.552 (3)	0.357 (3)	0.277 (3)	0.044 (5)
N4	0.8184 (2)	0.3098 (2)	0.3732 (2)	0.0430 (3)
H4*A*	0.867 (3)	0.443 (4)	0.314 (3)	0.058 (6)
H4*B*	0.862 (3)	0.227 (4)	0.317 (3)	0.059 (6)
O	0.7298 (2)	0.5611 (3)	0.86215 (19)	0.0541 (4)
H1*W*	0.749 (4)	0.442 (5)	0.912 (4)	0.077 (8)
H2*W*	0.769 (4)	0.622 (4)	0.919 (4)	0.081 (9)

The association of both maximum and minimum residual electron densities (0.49 and −0.52 e Å^{-3}, respectively) with H3 in the excess-electron-density map after several further cycles with this model, leading to R = 0.0304, $wR(F^2)$ = 0.0857, strongly suggested that these features resulted from the constraints. Removing them reduced the remaining densities significantly and improved R to 0.0268, $wR(F^2)$ to 0.0710, but resulted in significant departure of H3 from the N4—N3—C plane; see also §3.3. The stability of the refinement with H3 unrestrained suggested the testing of a completely free model in which x, y, z and U_{iso} were refined for all H atoms. The resulting refinement was found to be stable, giving reasonable parameter values associated with relatively large uncertainties as reported in Table 2.

Final refinement indicators for all reflections used are given in Table 1. The final difference Fourier map was essentially featureless with residual density that could not be interpreted further. Final atomic coordinates and equivalent isotropic displacement parameters for $CH_8N_4SiF_6$ are given in Table 2.

2.4. *Structure determination and refinement of bis[aminoguanidinium(1+)] hexafluorosilicate dihydrate*

A high percentage of the cleaved dihydrate crystals examined by X-ray diffraction proved to be twinned (see §2.5), although some small untwinned fragments were found. A colorless cleavage fragment was selected and mounted as in §2.3. See Table 1 for all other experimental details.

The structure was solved as in §2.3. The positions of all H atoms, including those of the water molecule, became clear from the difference Fourier distribution after a few cycles of refinement. H atoms were initially added to the model under constraints similar to those in §2.3; see Fig. 1(*b*) for the atomic labeling. Dimensions in the water molecule were initially taken as d_{O-H} = 0.82, $d_{H\cdots H}$ = 1.31 Å (*i.e.* H—O—H = 106.0°). Several cycles of refinement showed that extinction was significant, hence a refinable extinction parameter was again included; see §2.3 and Table 1.

The success of the model with fully refined H-atom parameters for the anhydrous material led to the use of a similar model for the dihydrate. Refinement was stable with reasonable parameter values, although those for the H atoms were again associated with relatively large uncertainties. The possibility that the tetrahedral geometry around N4 represented a local minimum in the error function was tested by refining several models with alternative N4 geometry. In each case, the final coordinates were indistinguishable from those reported in Table 3.

The final refinement indicators are given in Table 1. The final difference Fourier maps were essentially featureless, with only two maxima greater than 0.2 e Å^{-3}. These were associated with the SiF_6 group but were otherwise uninterpretable. Final atomic coordinates and equivalent isotropic displacement parameters for $(CH_7N_4)_2SiF_6{\cdot}2H_2O$ are presented in Table 3.

2.5. *Twinning in $(CH_7N_4)_2SiF_6{\cdot}2H_2O$*

Dihydrate crystals are generally found twinned, as noted in §2.4. The character of the twinning was determined by careful measurement of the setting angles of a

set of 50 reflections. The program *DIRAX* (Duisenberg, 1992) was used to analyze the relations in reciprocal space between these reflection angles for possible indexing. Two subsets, one containing 26 and the other containing 23 of these 50 reflections, could be indexed independently by use of the lattice dimensions given in Table 1. One reflection satisfied both lattices, and two (rather weak) reflections could not be indexed on either cell.

The program 2*VIEW* (described in the *DIRAX* manual) was used to calculate the transformation needed to bring one lattice into alignment with the other, based upon orientation matrices for the two lattices as input; the transformation required was a rotation of 180° about the *b* axis, consistent with the single reflection common to the two sets, $002/00\bar{2}$. Comparison of the indexed faces of the crystal used in the structure determination with other crystals observed as twinned under crossed polarizers revealed the composition plane for the twins to be (001). As $\gamma \simeq 90°$, lattice strain across this plane is minimized. The stress introduced by cleaving the crystal in preparation for X-ray measurement was observed to cause twinning in previously single-domain crystals.

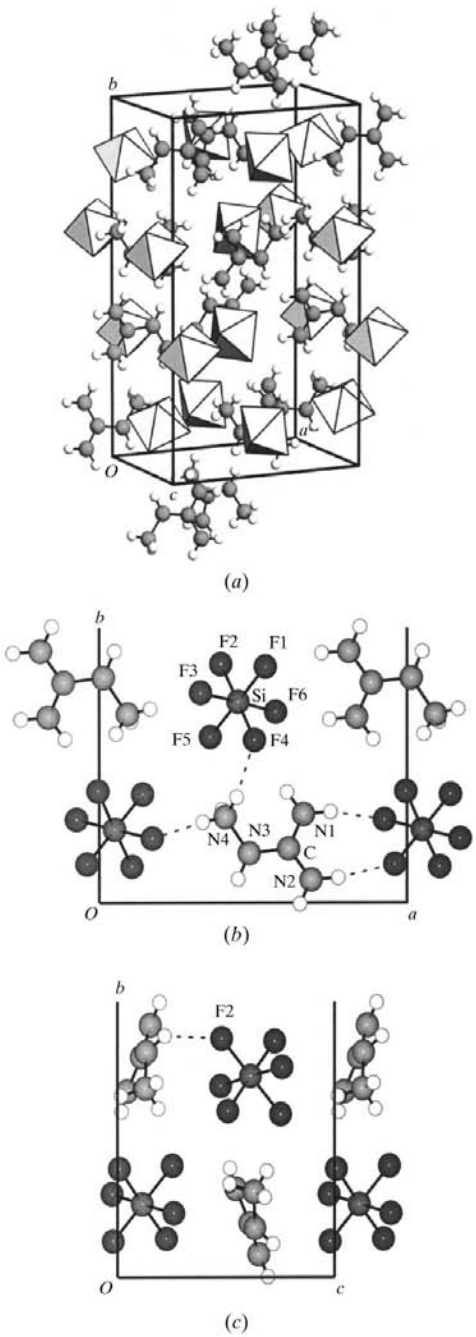

Fig. 2. (*a*) The content of the $CH_8N_4SiF_6$ unit cell at room temperature with octahedral SiF_6^{2-} ions depicted as solid polyhedra, the $CH_8N_4^{2+}$ cations by connected filled circles for C and N, open circles for H atoms. (*b*) The hydrogen-bond distribution in the $CH_8N_4SiF_6$ unit cell as viewed along the *c* axis from $z \simeq 0.3$ to 0.7 and $y = 0$ to $\frac{1}{2}$, with all atoms labeled. (*c*) The unit cell of $CH_8N_4SiF_6$ as viewed along the *a* axis from $x \simeq 0.3$ to 0.7 and $y = 0$ to $\frac{1}{2}$, illustrating the hydrogen bond between H3 and F2.

3. Structural results

3.1. *Crystal structure of $CH_8N_4SiF_6$*

The Si atom occupies a general position in the orthorhombic cell and is coordinated to six F atoms, forming a nearly ideal SiF_6 octahedron, see §3.4. Cations and anions in this structure pack together in a variant of the NaCl structure in which the SiF_6^{2-} and $CH_8N_4^{2+}$ ions alternate in intersecting rows parallel to each cell axis; see Fig. 2(*a*). The plane of the cation is approximately parallel to (001). The NH···F network present is illustrated by Figs. 2(*b*) and 2(*c*).

3.2. *Crystal structure of $(CH_7N_4)_2SiF_6{\cdot}2H_2O$*

The centrosymmetric triclinic unit cell contains a single dihydrate formula unit, with the Si atom located at the cell origin on an inversion center, see Table 3; the six coordinating F atoms form three sets of inversion-related pairs thereby forming the SiF_6^{2-} anion. The unique $CH_7N_4^+$ cation, with the C atom close to $\frac{1}{2}, \frac{1}{4}, \frac{1}{2}$ and the molecular plane approximately perpendicular to the *b* axis, forms infinite stacks along the *b* axis with head-to-tail packing of adjacent cations owing to the inversion center at the body center, see Figs. 3(*a*) and 3(*c*), and §3.5. The SiF_6^{2-} anions occupy columns between adjacent cation stacks, with the spacing between the anions double that between the cations for charge balance. The complete content of the unit cell lies close to (021), as seen in Fig. 3(*c*). Cleavage along this plane is hence expected and is indeed observed. Crystal elongation along [010], nearly perpendicular to (021), indicates this is a direction of fast crystal growth. The large number of hydrogen bonds formed as additional $CH_7N_4^+$ cations or

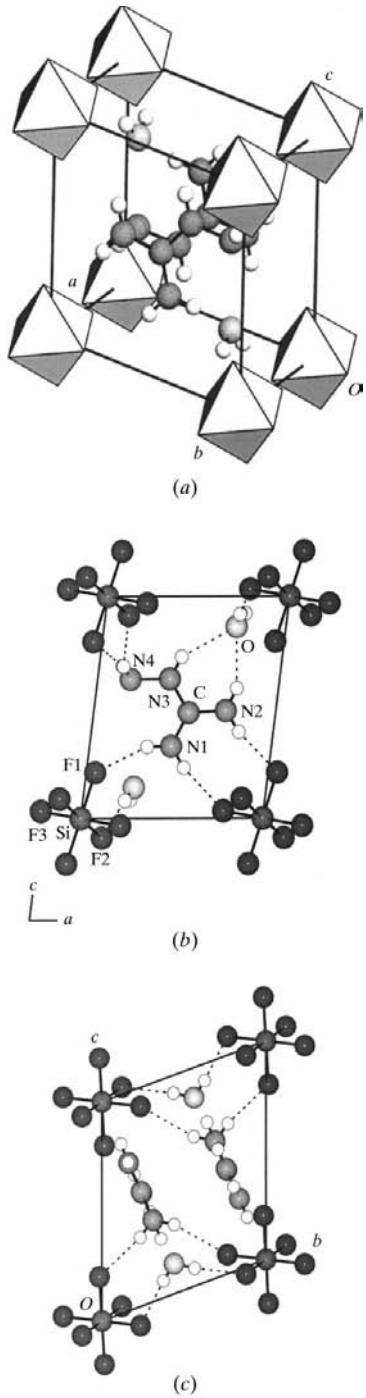

Fig. 3. (*a*) The content of the $(CH_7N_4)_2SiF_6{\cdot}2H_2O$ unit cell at room temperature with octahedral SiF_6^{2-} ions depicted as shaded solid polyhedra, the $CH_7N_4^+$ cations by connected filled circles for C and N, the H_2O molecules by closed circles for O, open circles for H atoms. (*b*) The hydrogen-bond distribution in the $(CH_7N_4)_2SiF_6{\cdot}2H_2O$ unit cell as viewed along the *b* axis from y = 0 to $\frac{1}{2}$, with all atoms labeled. (*c*) The arrangement of the $(CH_7N_4)_2SiF_6{\cdot}2H_2O$ unit-cell contents on (021), as viewed along the *a* axis. H4*A* and H4*B* are enlarged slightly for clarity.

SiF_6^{2-} anions occupy this plane (see §3.5) provides an attractive mechanism for fast crystal growth.

3.3. *Ammonioguanidinium(2+) and aminoguanidinium(1+) ions in $CH_8N_4SiF_6$ and $(CH_7N_4)_2SiF_6{\cdot}2H_2O$*

The single independent $CH_8N_4^{2+}$ cation in $CH_8N_4SiF_6$ is slightly but significantly nonplanar. The distance between C and the N1–N2–N3 plane is 0.011 (2) Å, with torsion angle N1—C—N3—N4 = 16.1 (2)°. In $CH_8N_4ZrF_6{\cdot}H_2O$ (Ross *et al.*, 1998), the corresponding out-of-plane distance is 0.013 (3) Å with a torsion angle of 19.9 (5)° in the first and 0.010 (4) Å and 5.8 (5)°, respectively, in the second independent cation. The nonplanar coordination about N3 owing to H3, see §2.3, is notable. Inspection of the Cambridge Structural Database (CSD) (1995; Allen *et al.*, 1991) reveals few structures in which such groups are significantly nonplanar; examination suggests most have reduced reliability in H-atom location. The out-of-plane displacement modifies the hydrogen-bonding pattern, allowing an approach of 2.12 (2) Å to F2, see Table 4; the resulting increase in structural stability supports this model. It may be emphasized that the position of H3 represents only the centroid of the associated electron density; the position of the nucleus is undetermined. The coordination geometry around N2 is regular, with $N2H_2$ essentially coplanar with the CN_3 core and bond angles near 120°, see Table 5; that about N1, however, is significantly distorted with a distance of 0.11 (2) Å from N1 to the C–H1*A*–H1*B* plane. This distortion decreases the distance, thus increasing the bond strength, between H1*A* and F6.

In contrast, although the three C—N distances in the dihydrate barely differ significantly from 1.322 Å, see Table 6, the $CH_7N_4^+$ cation remains accurately planar with an N1—C—N3—N4 torsion angle of 0.1 (2)° and a distance of 0.0021 (17) Å between C and the N1–N2–N3 plane. The sp^3 hybridization of N4, with its nearly single N4—N3 and two N—H bonds in the 1+ cation, was confirmed by the tests described in §2.4. Comparable results for the terminal N atom in another NH_2—N— group are reported by Akella & Keszler (1994); the CSD (1995; Allen *et al.*, 1991) also contains several reliable structures with similar geometry, including the neutron diffraction determination by Jeffrey *et al.* (1985) and X-ray studies by André *et al.* (1997), Bracuti (1986), Carugo *et al.* (1995) and Flippen-Anderson & Dudis (1989). A plot of the sum of the bond angles about the terminal N atom from the most reliable determinations of such groups in the CSD is narrowly distributed about 322°; sp^3 hybridization corresponds to 328.5° and a planar bond array to 360°. The coordination geometry around N1 and N2 is regular in the hydrate, with all NH_2 groups essentially coplanar with the CN_3 core and bond angles near 120°.

Table 4. *H···F and H···O distances (Å), hydrogen-bond valences (v.u.), X···Y distances (Å) and X—H···Y angles (°) in $CH_8N_4SiF_6$ and $(CH_7N_4)_2SiF_6{\cdot}2H_2O$*

$CH_8N_4SiF_6$	H···F	Bond valence†	N···F	Angle	$(CH_7N_4)_2SiF_6{\cdot}2H_2O$	H···F,O	Bond valence†	O,N···F,O	Angle
N1—H1*A*···F6	1.96 (3)	0.11 (1)	2.803 (2)	173 (2)	O—H2*W*···F2	2.07 (3)	0.091 (5)	2.840 (2)	175 (3)
N1—H1*B*···F4	2.17 (3)	0.077 (4)	2.861 (2)	145 (3)	O—H1*W*···F3	2.07 (3)	0.091 (5)	2.846 (2)	174 (3)
N2—H2*A*···F1	2.11 (3)	0.085 (4)	2.931 (2)	152 (2)	N2—H2*B*···O	2.11 (2)	0.102 (4)	2.886 (2)	155 (2)
N2—H2*B*···F3	2.18 (3)	0.075 (4)	2.903 (2)	150 (2)	N3—H3···O	2.24 (2)	0.081 (3)	2.978 (2)	149 (2)
N3—H3···F1	2.43 (2)	0.052 (2)	3.048 (2)	141 (2)	N1—H1*B*···F1	2.21 (2)	0.072 (2)	2.935 (2)	155 (2)
N4—H4*B*···F3	1.85 (3)	0.140 (8)	2.746 (2)	179 (2)	N1—H1*A*···F3	2.28 (2)	0.064 (2)	3.089 (2)	152 (2)
N4—H4*A*···F3	2.30 (2)	0.062 (2)	2.992 (2)	143 (2)	N2—H2*A*···F1	2.05 (2)	0.095 (4)	2.907 (2)	164 (2)
N4—H4*C*···F4	1.93 (3)	0.120 (6)	2.831 (2)	166 (2)	N4—H4*A*···F2	2.31 (2)	0.062 (2)	3.142 (2)	153 (2)
N3—H3···F2	2.21 (2)	0.072 (2)	2.823 (2)	141 (2)	N4—H4*B*···F1	2.36 (3)	0.057 (3)	3.186 (2)	166 (2)

† For bonds with strength greater than 0.05 v.u.

Table 5. *Selected geometric parameters (Å, °) for $CH_8N_4SiF_6$*

Si—F2	1.6684 (9)	Si—F5	1.6727 (8)
Si—F1	1.6761 (8)	Si—F6	1.6813 (9)
Si—F3	1.7034 (9)	Si—F4	1.7043 (9)
C—N2	1.300 (2)	C—N1	1.309 (2)
C—N3	1.3632 (19)	N1—H1*A*	0.85 (3)
N1—H1*B*	0.80 (3)	N2—H2*A*	0.89 (3)
N2—H2*B*	0.80 (3)	N3—N4	1.4203 (17)
N3—H3	0.74 (2)	N4—H4*A*	0.82 (2)
N4—H4*B*	0.90 (3)	N4—H4*C*	0.92 (3)
F2—Si—F5	90.11 (5)	F2—Si—F1	90.87 (5)
F5—Si—F1	178.29 (5)	F2—Si—F6	91.86 (5)
F5—Si—F6	90.30 (5)	F1—Si—F6	91.07 (5)
F2—Si—F3	90.05 (5)	F5—Si—F3	89.76 (5)
F1—Si—F3	88.84 (5)	F6—Si—F3	178.09 (5)
F2—Si—F4	178.48 (5)	F5—Si—F4	89.26 (4)
F1—Si—F4	89.72 (5)	F6—Si—F4	89.53 (5)
F3—Si—F4	88.56 (5)	N2—C—N1	121.24 (14)
N2—C—N3	117.48 (14)	N1—C—N3	121.25 (13)
C—N1—H1*A*	116.7 (15)	C—N1—H1*B*	118 (2)
H1*A*—N1—H1*B*	121 (3)	C—N2—H2*A*	117.8 (15)
C—N2—H2*B*	119.2 (18)	H2*A*—N2—H2*B*	123 (2)
C—N3—N4	117.80 (12)	C—N3—H3	114.5 (15)
N4—N3—H3	112.2 (15)	N3—N4—H4*A*	107.8 (15)
N3—N4—H4*B*	107.3 (14)	H4*A*—N4—H4*B*	106 (2)
N3—N4—H4*C*	116.4 (15)	H4*A*—N4—H4*C*	109 (2)
H4*B*—N4—H4*C*	111 (2)		

All other bond distances and angles in the cations of both materials are normal, as shown in Tables 5 and 6.

3.4. *Hexafluorosilicate ions in $CH_8N_4SiF_6$ and $(CH_7N_4)_2SiF_6{\cdot}2H_2O$*

The Si—F bond lengths in $CH_8N_4SiF_6$ range from 1.6684 (9) to 1.7043 (9) Å with <Si—F> = 1.684 (16) Å, twelve F—Si—F angles range from 88.56 (5) to 91.86 (5)° with <F—Si—F> = 90.0 (9)°, see Table 5. The octahedral-distortion indicators (Robinson *et al.*, 1972) are indicative of a nearly regular SiF_6 octahedron, with quadratic elongation factor $\lambda = \sum_{i=1}^{6}(l_i/l_0)^2/6 = 1.00034\ (2)$ and angle variance $\sigma^2_{\theta(\mathrm{oct})} = \sum_{i=1}^{12}(\theta_t - 90^\circ)^2/11 = 0.89\ (5)^\circ$, where l_i and l_0 are Si—F lengths in the strained and unstrained states and θ_i is the *i*th octahedral angle. Corresponding distortion values for an ideal octahedron are unity and zero, respectively; the present octahedral volume is 6.369 (4) Å^3. Several inter-octahedral F···F distances form in the range 2.942 (1)–3.218 (2) Å. These contacts correspond to close anion–anion approaches in the underlying NaCl structure, *i.e.* between octahedra related by the [110] vector or its equivalents in a distortion of the ideal structure.

The SiF_6 octahedron in $(CH_7N_4)_2SiF_6{\cdot}2H_2O$ is even closer to ideal, with bond lengths ranging from 1.6797 (9) to 1.6808 (9) Å and <Si—F> = 1.6801 (6) Å; the F—Si—F angles range from 89.26 (5) to 90.76 (5)° with <F—Si—F> = 90.0 (7)°, see Table 6. The quadratic elongation factor $\lambda = 1.00013\ (1)$ and angle variance $\sigma^2_{\theta(\mathrm{oct})} = 0.45\ (4)^\circ$ also indicate a nearly regular octahedron; the corresponding volume is 6.322 (6) Å^3, slightly smaller than that in $CH_8N_4SiF_6$.

3.5. *Role of the water molecule in $(CH_7N_4)_2SiF_6{\cdot}2H_2O$*

The structure of $(CH_7N_4)_2SiF_6{\cdot}2H_2O$ results from a balance between four or more sets of forces: (i) coulombic attraction between SiF_6^{2-} and $CH_7N_4^+$ ions; (ii) coulombic repulsion between adjacent $CH_7N_4^+$ ions; (iii) formation of hydrogen bonds between ions; (iv) stabilization effects owing to H_2O. The first force leads to a unit cell in which two completely contained cations are surrounded by corner-sharing SiF_6^{2-} anions. The arrangement of anions around the cations is highly non-uniform, however, with the coordinating F1 and F3 atoms very nearly in the same plane as N1 and N2 [the maximum planar deviation is 0.219 (1) Å for N1] to which the F1, F2, N4 plane is inclined by 67.81 (3)°, see Figs. 3(*b*) and 3(*c*). The second force tends to destabilize the structure. Although adjacent cation columns appear to be effectively screened from each other by the intervening anions, such screening may be less effective along the *b* axis. The balance between repulsive forces and the extensive hydrogen-bond system is most likely the cause of the easy cleavage along (021). The dimensions of the hydrogen bonds formed between $CH_7N_4^+$ and SiF_6^{2-}, between H_2O and SiF_6^{2-}, and between $CH_7N_4^+$ and H_2O are given in Table 4.

Table 6. *Selected geometric parameters (Å, °) for* $(CH_7N_4)_2SiF_6{\cdot}2H_2O$

Si—F1	1.6797 (9)	Si—F2	1.6798 (9)
Si—F3	1.6808 (9)	C—N1	1.313 (2)
C—N2	1.324 (2)	C—N3	1.329 (2)
N1—H1*A*	0.89 (2)	N1—H1*B*	0.781 (19)
N2—H2*A*	0.88 (2)	N2—H2*B*	0.83 (2)
N3—N4	1.4037 (19)	N3—H3	0.83 (2)
N4—H4*A*	0.90 (2)	N4—H4*B*	0.85 (2)
O—H1*W*	0.78 (3)	O—H2*W*	0.77 (3)
F1—Si—F2	90.35 (5)	F1—Si—F3	89.26 (5)
F2—Si—F3	90.76 (5)	N1—C—N2	121.27 (15)
N1—C—N3	120.98 (14)	N2—C—N3	117.75 (15)
C—N1—H1*A*	119.6 (12)	C—N1—H1*B*	120.4 (13)
H1*A*—N1—H1*B*	119.8 (19)	C—N2—H2*A*	123.3 (14)
C—N2—H2*B*	118.3 (14)	H2*A*—N2—H2*B*	118.3 (19)
C—N3—N4	119.85 (14)	C—N3—H3	119.0 (13)
N4—N3—H3	121.1 (13)	N3—N4—H4*A*	106.8 (13)
N3—N4—H4*B*	105.1 (15)	H4*A*—N4—H4*B*	111 (2)
H1*W*—O—H2*W*	105 (3)		

Fig. 3(*b*) shows the arrangement of a $CH_7N_4^+$ ion and two H_2O molecules with respect to a plane defined by four SiF_6^{2-} groups. The orientation of the $CH_7N_4^+$ ion allows the molecule to form N—H···F bonds to three of these SiF_6^{2-} groups but not to the fourth. The presence of water in the structure allows that fourth SiF_6^{2-} group to be hydrogen-bonded through water to $CH_7N_4^+$. Further, as seen in Fig. 3(*c*), the split hydrogen-bond network illustrated by N4—H4*A*···F2 and N4—H4*B*···F1 is echoed in the linkages O—H1*W*···F3 and O—H2*W*···F2. If the water molecule were removed, both an enthalpic (hydrogen-bond breaking) and entropic (reduced constraints on aminoguanidinium) penalty would ensue. The presence of the water molecule is hence essential to structural stability.

The striking difference in density between $(CH_7N_4)_2SiF_6{\cdot}2H_2O$, D_m = 1.67 (1) Mg m^{-3}, and anhydrous $CH_8N_4SiF_6$, D_m = 2.11 (3) Mg m^{-3}, results partly from the additional lower-density $CH_7N_4^+$ cation and water molecule in the former and partly from differences in the strength of the hydrogen bonds formed by the water as compared with cation···H bonds. The relative importance of these factors may be judged by estimating the void space in the two structures, *i.e.* the proportion of unit-cell volume outside the van der Waals radius of any atom. Assuming van der Waals radii of 2.2 Å for Si, 1.3 Å for F, 1.55 Å for C, 1.40 Å for N, 1.35 Å for O and 1.10 Å for H, 39.9% of the hydrate structure and 31.8% of the anhydrous structure are void. A hypothetical $CH_8N_4SiF_6$ structure in which 39.9% void space was inserted would have a density of 1.86 Mg m^{-3}, a decrease of 0.25 Mg m^{-3} from D_m but still 0.19 Mg m^{-3} greater than D_m[$(CH_7N_4)_2SiF_6{\cdot}2H_2O$]. The increased packing efficiency (governed to a large extent by the hydrogen-bonding network) hence accounts for more than half the density difference between the two structures; the balance results from the higher 'average atomic weight' ($M_r/\sum_a N_a$) of $CH_8N_4SiF_6$. All relevant hydrogen-bond lengths, angles and strengths are given in Table 4.

3.6. *Influence of preparation on composition*

Minor changes in the relative concentration and temperature of the reactants in solution result in a wide variety of final compositions. An outline of the role played by the primary variables has been given by Ross *et al.* (1999). A fuller discussion of these variables and their resulting chemistry has been presented by Bauer *et al.* (1999).

4. Discussion

Direct comparison of the $CH_8N_4SiF_6$ and $CH_8N_4ZrF_6$ structures is complicated by their very different atomic arrangements; the former contains isolated SiF_6^{2-} anions, the latter distorted antiprisms of edge-sharing ZrF_8^{4-} polyhedra with <Zr—F> = 2.12 (13) and 2.12 (11) Å for the two independent units (Bukvetskii *et al.*, 1989). The formation of isolated ZrF_6^{2-} octahedra in $(CH_7N_4)_2ZrF_6$, with <Zr—F> = 2.005 (7) Å as reported by Bukvetskii *et al.* (1989), shows the ionic radius of Si to be 0.32 Å smaller than that of Zr, in close accord with the difference between the Si^{4+} and Zr^{4+} ionic radii, 0.54 and 0.86 Å, respectively, given by Shannon (1976).

Comparable dimensions within $CH_7N_4^+$ and $CH_8N_4^{2+}$ cations previously reported in various zirconates do not differ significantly, see Figs. 4(*a*) and (*b*), and §1; uncertainties here are calculated from the reported dispersion by Bessel's method. The smaller uncertainties

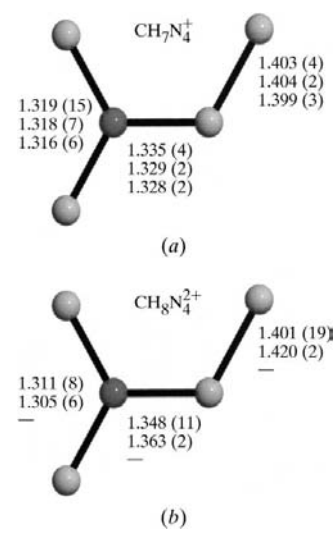

Fig. 4. Variation of (*a*) aminoguanidinium(1+) and (*b*) ammonioguanidinium(2+) bond lengths (Å) as a function of the counterion. Upper values refer to zirconates, middle values to silicates, and lower values in (*a*) only to nitrates.

in the fluorosilicates reveal a significant increase in central C—N and N—N distances from the 1+ to the 2+ cation, whereas the terminal C—N bonds do not differ significantly. Akella & Keszler's (1994) C—N and N—N distances in $CH_7N_4^+{\cdot}NO_3^-$ agree well with the present work, see Fig. 4(*a*).

Evidence for rather linear N1—H1*A*···F6 and N4—H4*B*···F3 cation–anion interactions in $CH_8N_4SiF_6$, with potential hydrogen bonds as short as 1.85 Å corresponding to bond valences of 0.140 (8) v.u., and a highly nonlinear N2—H2*A*···F1 interaction of 2.11 Å with a bond valence of 0.085 (4) v.u. (Brown & Altermatt, 1985), is provided in Table 4. These values allow minimum estimates of the hydrogen-bond strengths; Brown & Altermatt (1985) have suggested that measured N—H or O—H distances be increased to ~1.0 Å, as a correction to the electron-density-centroid approximation for H-atom positions determined by X-ray diffraction, before acceptor···H distances are estimated. The relatively weak hydrogen bonds shown in Table 4 and in Figs. 2(*b*), 2(*c*), 3(*b*) and 3(*c*), as well as many others of strength less than 0.05 v.u., represent a major contribution to the enthalpy of the two materials.

Participation in this work by MRB, a senior undergraduate student at Southern Oregon University, forms part of the requirements for his BS degree. Support of this research by the National Science Foundation (DMR-9708246) and, in part, by Cancer Center Support CORE Grant P30 CA 21765 is gratefully acknowledged as is that of the American Lebanese Syrian Associated Charities (ALSAC) by CRR. The helpful comments of a referee leading to improved clarity of this paper are highly appreciated.

References

Akella, A. & Keszler, D. A. (1994). *Acta Cryst.* C**50**, 1974–1976.
Alcock, N. W. & Marks, P. J. (1994). *J. Appl. Cryst.* **27**, 200.
Allen, F. H., Davies, J. E., Galloy, J. J., Johnson, O., Kennard, O., Macrae, C. F., Mitchell, E. M., Mitchell, G. F., Smith, J. M. & Watson, D. G. (1991). *J. Chem. Inf. Comput. Sci.* **31**, 187–204.
André, C., Luger, P., Fuhrhop, J.-H., & Hahn, F. (1997). *Acta Cryst.* B**53**, 490–497.
Bauer, M. R., Ross, C. R. II, Nielson, R. M. & Abrahams, S. C. (1999). *Inorg. Chem.* In the press.
Bracuti, A. J. (1986). *Acta Cryst.* C**42**, 1887–1889.
Brown, I. D. & Altermatt, D. (1985). *Acta Cryst.* B**41**, 244–247.
Bukvetskii, B. V., Gerasimenko, A. V. & Davidovich, R. L. (1989). *Koord. Khim.* **15**, 130–135.
Bukvetskii, B. V., Gerasimenko, A. V. & Davidovich, R. L. (1990). *Koord. Khim.* **16**, 1479–1484.
Bukvetskii, B. V., Gerasimenko, A. V. & Davidovich, R. L. (1992). *Koord. Khim.* **18**, 576–579.
Bukvetskii, B. V., Gerasimenko, A. V., Kondratyuk, I. P., Davidovich, R. L. & Medkov, M. A. (1987). *Koord. Khim.* **13**, 661–668.
Burla, M. C., Camalli, M., Cascarano, G., Giacovazzo, C., Polidori, G., Spagna, R. & Viterbo, D. (1989). *J. Appl. Cryst.* **22**, 389–393.
Burnett, M. N & Johnson, C. K. (1996). *ORTEP*III. Report ORNL-6895. Oak Ridge National Laboratory, Oak Ridge, Tennessee, USA.
Cambridge Structural Database (1995). *User's Manual.* Version 5.10. Cambridge Crystallographic Data Centre, 12 Union Road, Cambridge, England.
Carugo, O., Castellani, C. B. & Perotti, A. (1995). *Acta Cryst.* C**51**, 1683–1687.
Duisenberg, A. J. M. (1992). *J. Appl. Cryst.* **25**, 92–96.
Enraf–Nonius (1988). *CAD*-4 *Diffractometer Reference Manual.* Delft Instruments X-ray Diffraction BV, Delft, The Netherlands.
Flippen-Anderson, J. L. & Dudis, D. S. (1989). *Acta Cryst.* C**45**, 1107–1109.
Gerasimenko, A. V., Kondratyuk, N. P., Davidovich, R. L., Medkov, M. A. & Bukvetskii, B. V. (1986). *Koord. Khim.* **12**, 710–714.
Harms, K. (1997). *XCAD*-4. *Program for the Lp Correction of Nonius CAD*-4 *Diffractometer Data.* University of Marburg, Germany.
Jeffrey, G. A., Ruble, J. R., Nanni, R. G., Turano, A. M. & Yates, J. H. (1985). *Acta Cryst.* B**41**, 354–361.
Robinson, K., Gibbs, G. V. & Ribbe, P. H. (1972). *Science*, **172**, 567–570.
Ross, C. R. II, Paulsen, B. L., Nielson, R. M. & Abrahams, S. C. (1998). *Acta Cryst.* B**54**, 417–423.
Ross, C. R., Pugmire, D. L., Nielson, R. M. & Abrahams, S. C. (1999). In preparation.
Shannon, R. D. (1976). *Acta Cryst.* A**32**, 751–767.
Sheldrick, G. M. (1997). *SHELX*97.1 *Users' Manual.* University of Göttingen, Germany.
Waters, T. N. (1960). *J. Inorg. Nucl. Chem.* **15**, 320–328.